III. 研究成果の刊行に関する一覧表

雑誌

発表者氏名	論文タイトル	発表誌名	巻号	ページ	出版年
Miyazawa M Ishii T Kirinashizawa M Yasuda K, Hino O Hartman PS Ishii N	Cell growth of the mouse SDHC mutant cells was suppressed by apoptosis throughout mitochondrial pathway,	BioScience Trends	2	22-30	2008
Yamaguchi T Onodera A Yasuda K Nishio Y Arai M Tsuda M Miyazawa M Hartman PS Ishii N	A low cost and quick assay system using the free-living nematode *Caenorhabditis elegans* to determine the effects of Kampo medicine on life span	AATEX	13	1-10	2008
Ishii N, Ishii T, Hartman PS	The role of the electron transport SDHC gene on lifespan and cancer,	Mitochondrion	7	24-28	2007
Tuda M Sugiura T Ishii T Ishii N Aigaki T	A *mev-1* life dominant-negative SdhC increases oxidative stress and reduces lifespan in *Drosophila*,	Biochem. Biophys. Res. Com.	363	342-346	2007
Ishii N	Role of oxidative stress from mitochondria on aging and cancer,	Cornea	26	S3-S9	2007
Sakashita T Hamada N Suzuki M Ikeda DD Yanase S Ishii N Kobayashi Y	: Effects of γ-ray irradiation on olfactory adaptation to benzaldehyde in *Caenorhabditis elegans*,	Biological Sciences in Space	21	117-120	2007
Sakashita T Hamada N Ikeda DD Yanase S Suzuki M Ishii N Kobayashi Y	Modulatory effect of ionizing radiation on food-NaCl associated learning: the role of γ subunit of G protein in *Caenorhabditis elegans*,	FASEB J.	22	713-720	2007
石井直明	寿命および寿命関連遺伝子	医学のあゆみ	222	299-303	2007
石井直明 桑平一郎（監修）	専門医がやさしく教える老化予防＆アンチエイジング	ＰＨＰ出版			2007

Ohta K Shigemoto K Fujinami A Maruyama N, Konishi T Ohta M	Clinical and experimental features of MuSK antibody positive MG in Japan.	Eur J Neurol	14	1029-1034	2007
Ishigami A Maruyama N	Significance of SMP30 in gerontology.	Geriatr Gerontol Int	7	316-325	2007
Kimura Y Kubo S Koda H Noguchi Y Sawabe M Maruyama N Kitamura K 127:1024-1030, 2007	Quantitative analysis of mRNA in human temporal bones.	Acta Otolaryngol.	127	1024-1030	2007
丸山直記 重本和宏	神経筋接合部位における抗 MuSK 抗体と病態機序	臨床神経	47	842-844	2007
佐藤　匡 瀬山邦明 石神昭人 丸山直記	肺の老化のメカニズム	The Lung Perspectives	15	155-160	2007

IV. 研究成果の刊行物

Original Article

Cell growth of the mouse SDHC mutant cells was suppressed by apoptosis throughout mitochondrial pathway

Masaki Miyazawa[1,*], Takamasa Ishii[1,*], Mika Kirinashizawa[1], Kayo Yasuda[1], Okio Hino[2], Philip S. Hartman[3], Naoaki Ishii[1,]**

[1] *Department of Molecular Life Science, Division of Basic Medical Science and Molecular Medicine, Tokai University School of Medicine, Isehara, Kanagawa, Japan;*
[2] *Department of Pathology (II), Juntendo University School of Medicine, Bunkyo-ku, Tokyo, Japan;*
[3] *Department of Biology, Texas Christian University, Fort Worth, Texas, USA.*

Summary **SDHC E69 cells, which overproduce superoxide anions in their mitochondria, were previously established that had a mutation in the SDHC gene of complex II of the respiratory chain. We now demonstrate that tumors formed by NIH 3T3 and SDHC E69 cells showed significant histological differences. Cytoplasmic cytochrome c release from mitochondria was significantly elevated in SDHC E69 cells and was likely caused by superoxide anion overproduction from mitochondria. In addition, the p53 and Ras signal transduction pathways were activated by oxidative stress and may play a key role in the supernumerary apoptosis in SDHC E69 cells. Our results suggest that the development and growth characteristics of hereditary paragangliomas, which are defective in the same complex of electron transport as mouse SDHC E69 cells, may be caused by apoptosis induction by mitochondrial oxidative stress.**

Keywords: Mitochondria, Superoxide anion, Oxidative stress, Apoptosis, Paraganglioma

1. Introduction

Major endogenous reactive oxygen species (ROS) are generated from electron leakage during cellular respiration in mitochondria (*1*). The *mev-1* mutant of the nematode *Caenorhabditis elegans* is mutated in the SDHC subunit of complex II in electron transport system (*2*) and produces excessive superoxide anions (O_2^-) in its mitochondria (*3*). This mutant has proven extremely useful for the study of endogenous oxidative stress and its effects on lifespan, apoptosis and mutagenesis (*4,5*). We have recently constructed a transgenic mouse cell line (SDHC E69 cells) with a mutation that mimics *mev-1* (*6*). As in *C. elegans*, excess O_2^- were generated, which led to supernumerary apoptosis and hypermutability (*6*). Interestingly, the SDHC E69 cells that escaped from apoptosis were frequently transformed and, when the cells were injected under the epithelium of nude mice, they resulted in the production of tumors two weeks after implantation (*6*). Conversely, after wild-type cells (NIH3T3 cells) were injected, they were on the verge of disappearance but were transformed at high frequency by spontaneous mutations during long passage time or culture time. We show in this report that the NIH3T3 wild-type tumors developed with considerable proliferative abilities over the course of further incubation while the tumor mass of SDHC E69 transformed cells did not significantly enlarge.

It has been reported that mutations in the SDHC or SDHD gene of mitochondrial complex II cause some nonchromaffin and hereditary paragangriomas (PGLs) in humans (*7,8*). Therefore, further analysis of SDHC E69 cells may help clarify the molecular mechanism of the tumorigenesis in neoplasms such as PGLs. It is clear that apoptosis and cell-cycle arrest serve as defensive mechanisms to rid organisms from potentially neoplastic cells. However, the molecular mechanisms by which apoptosis is stimulated by ROS overproduction

*These authors contributed equally to this work.
***Correspondence to:* Dr. Naoaki Ishii, Department of Molecular Life Science, Division of Basic Medical Science and Molecular Medicine, Tokai University School of Medicine, 143 Shimokasuya, Isehara, Kanagawa 259-1193, Japan;
e-mail: nishii@is.icc.u-tokai.ac.jp

from mitochondria are not completely understood. In this report, we explored the mitochondrial and cytosolic responses on apoptosis to ROS overproduction in SDHC E69 mitochondria. Specifically, excess apoptosis in SDHC E69 cells was mediated virtually exclusively through the mitochondrial pathway. In addition, p53 and Ras-MEKK pathways were presumably stimulated in the SDHC E69 cells.

2. Materials and Methods

2.1. *Cell culture*

The cells were cultivated in DMEM medium (Nissui Company, Tokyo) including 2.5% FBS + 2.5% CS in a 5% CO_2 incubator. Cell division and proliferation were examined after synchronous culture in G0 phase into exhaustion of serum medium and at the contact inhibition state in 100-mm tissue culture dishes. For cell growth, 5×10^4 synchronized cells were cultured in a standard medium of 35-mm tissue culture dishes.

In this manuscript, three-month SDHC E69 cells after the establishment and their wild-type cells (NIH3T3 cells) for 3 month cultured cells as progenitors were used. In brief, the three-month SDHC E69 cells showed the loss of contact inhibition and had many apoptotic molecule-like granules during the first month after establishment (*6*). During the period of colony formation, some clefts characteristics of programmed cell death were found in the center of some colonies (*6*). In the SDHC E69 cells, the morphology was changed from the typical solid and elongated fibroblasts to smooth and rounded cells (*6*). Similar changes were evident, although to a lesser degree in the one-month SDHC E69 cells after establishment (*6*). In addition, the three-month SDHC E69 cells formed multiple layers (*6*).

2.2. *Antibodies and chemicals*

Caspase inhibitors *Z*-Leu-Glu(OMe)-Thr-Asp-(OMe)-FMK (an inhibitor of caspase 8) and *Z*-Leu-Glu(OMe)-His-Asp(OMe)-FMK (an inhibitor of caspase 9) were purchased from ICN Pharmaceuticals (Irvine). p53 antibody, phospho-p53 (Ser15) antibody, phospho-p38 MAP kinase (Thr180/Tyr182) antibody, phospho-SAPK/JNK (Thr183/Tyr185) antibody and Bid antibody were purchased from Cell Signaling Technology. p21 (C-19) antibody, Bax (N-20) antibody and MEK kinase-1 (C-22) were purchased from Santa Cruz Biotechnology, Inc (Santa Cruz). Anti-cytochrome c monoclonal antibody was purchased form BD PharMingen (San Jose). Anti-rabbit Ig, horseradish peroxidase linked $F(ab')_2$ fragment (from donkey) and anti-mouse Ig, horseradish peroxidase linked $F(ab')_2$ fragment (from sheep) were purchased from Amersham Pharmacia Biotech. The luciferase reporter gene pp53-TA-Luc and pTA-Luc vector used in the p53 reporter assay were purchased from Clontech.

2.3. *Transfection and luciferase assay*

An AP-1 cis-element dependent transcriptional expression vector (pAP-1-TA-Luc) was constructed using the AP-1 cis-element 5' primer (CTAGCTGAGT CAGTGAGTCACTGACTCACTGACTCATGAGTCA GCTGACTCA) and the AP-1 cis-element 3' primer (G ATCTGAGTCAGCTGACTCATGAGTCAGTGAGTC AGTGACTCACTGACTCAG). These were annealed, and this oligonucleotide was inserted at an *NheI-BglII* site in the pE2F-TA-Luc plasmid vector without the E2F binding site. A pE2F-TA-Luc plasmid vector without the E2F binding site (p-TA-Luc) was used as the negative control vector. Transient transfection of pp53-TA-Luc (0.5 μg), pTA-Luc (0.5 μg) and pCMV-β-galactosidase (0.05 μg) or pAP-1-TA-Luc (0.5 μg), p-TA-Luc (0.5 μg) and pCMV-β-galactosidase (0.05 μg) into NIH3T3 and SDHC E69 cell lines was performed using LipofectAMINE Plus reagent (Invitrogen Inc.). Proteins were prepared for luciferase and β-galactosidase analysis 48 h after transfection by addition of lysis buffer (0.625 mM Tris-PO_4 (pH 7.8), 15% glycerol, 2% CHAPS, 1% Lecichin (*L*-α-phosphachigilcholine), 1% BSA, 0.1 M EGTA, 1 M $MgCl_2$, 1 M DTT, 0.1 M *p*-APMSF). These protein lysates were measured for luciferase and β-galactosidase activities using Luminescencer-PSN (ATTO) or SPECTRA MAX 250 (Molecular Devices) after addition of luciferese buffer (20 mM Tricine-NaOH, 1 mM $4MgCO_2 \cdot Mg(OH) \cdot 5H_2O$ (pH 2.3), 2.7 mM $MgSO_4 \cdot 7(H_2O)$ (pH 2.3), 0.1 mM EDTA, 33 mM DTT, 0.27 mM CoA-Li, 0.47 mM luciferin, 0.53 mM ATP)) or β-galactosidase buffer (60 mM $Na_2HPO_4 \cdot 12H_2O$, 10 mM KCl, 1 mM $MgCl_2$, 40 mM $NaH_2PO_4 \cdot 2H_2O$, 1.1 mM ONPG, 47.5 mM 2-mercaptoethanol). Samples were then incubated for 1 h at 37°C. Luciferase relative activity was normalized based on β-galactosidase activity levels and luciferase activity levels of p-TA-Luc, pTA-Luc negative control vector.

2.4. *Northern blot analysis*

Mouse cDNA's for Northern blot analysis were obtained by RT-PCR method using oligonucleotides for MDM2 (5'-GCC ACC AGA AGA GAA ACC-3' and 5'-GCC TGA GCT GAG TTT TCC-3'), p21-Ras (5'-TTG GAG CAG GTG GTG TTG-3' and 5'-ACA CAT CAG CAC ACA GGG-3'), M-Ras (5'-AGT AGT GGT GGG AGA TGG-3' and 5'-AGT TTG TGA GTG CCG GTG-3'), Raf-1/C-Raf (5'-CAT GAG CAC TGT AGC ACC-3' and 5'-ATC TCC ATG CCA CTT GCC-3'), 18s rRNA (5'-TAC CTG GTT GAT CCT GCC-3' and 5'-TTT CGT CAC TAC CTC CCC-3'), actin (5'-TGG AGA AGA TCT GGC ACC-3' and 5'-ACC CAA GAA GGA AGG CTG-3'), and G3PDH (5'-CAC GGC AAA TTC AAC

GGC-3' and 5'-CTT GGC AGG TTT CTC CAG-3'). 3 μg of mRNA which was extracted by Oligotex-dT30 Super (Roche) was subjected to Northern Blot analysis. Mouse cDNA's were random-prime-labeled using the High prime kit (Roche) with ^{32}P-dCTP (Amersham Biosciences) and purified using ProbeQuant G-50 Micro Columns (Amersham Biosciences). After hybridization for mouse cDNA's filters were stripped and reprobed for actin and G3PDH to verify that comparable amounts of RNA had been loaded in all lanes.

2.5. *Western blot analysis*

After a particular treatment, cells were washed twice with phosphate buffered saline and incubated on ice in lysis buffer containing 10 mM Tris-HCl (pH 8.0), 1 mM EDTA, 100 mM NaCl, 0.1% NP-40, 1 mM DTT and 0.1 mM *p*-APMSF for 10 min. This was followed by brief sonication for Western blot analysis of p53 or p21. Cell lysates for p21 analysis were then cleared by centrifugation (400 × *g*) for 5 min, and the supernatants were used. In Western blot analysis of Bax or cytochrome c, both the mitochondrial and cytoplasm fractions were employed. These cell lysates (containing 10-100 μg of protein) were solubilized by boiling after the addition of 2 × SDS-PAGE sample buffer (0.125 M Tris-HCl (pH 6.8), 10% 2-mercaptoethanol, 4% SDS, 10% sucrose and 0.004% bromophenol blue). For the analysis of p38, p-JNK, Bid or MEKK1, cells were washed twice with phosphate buffered saline and incubated in SDS-PAGE sample buffer containing 62.5 mM Tris-HCl (pH 6.8), 2% SDS, 50 mM DTT and 10% glycerol for 10 min on ice followed by brief sonication. Cell lysates were then cleared by centrifugation (400 × *g*) for 5 min and the supernatants were directly subjected to SDS-PAGE. After electrophoresis, the proteins were transferred to PVDF (polyvinyliden difluoride) membrane Clearblot membrane (ATTO) using a Semi-dry blotting machine AE-6677 (ATTO). To block nonspecific protein binding, membranes treated for 8 h at 20-25°C with either 0.1% Tween 20, 5% nonfat dried milk in phosphate buffered saline for analyses of p53, p21, Bax, cytochrome c, Bid or MEKK1 or 5% bovine serum albumin, 0.1% Tween 20 in TBS (0.02 M Trizma base, 0.137 M NaCl (pH 7.6)) for analyses of phospho-p53 (Ser15), phospho-p38 MAP kinase (Thr180/Tyr182) or phospho-SAPK/JNK (Thr183/Tyr185). The membranes were treated with anti- p53, p21, Bax, cytochrome c, or MEKK1 antibody in phosphate buffered saline containing 0.1% Tween 20, 5% nonfat dried milk, or phospho-p53 (Ser15) antibody in TBS containing 0.1% Tween 20, 5% bovine serum albumin at room temperature for 1 h or with Bid antibody in phosphate-buffered saline containing 0.1% Tween20, 5% nonfat dried milk, or phospho-p38 MAP kinase (Thr180/Tyr182) or phospho-SAPK/JNK (Thr183/Tyr185) antibody in TBS containing 0.1% Tween 20, 5% bovine serum albumin at 4°C for 8 h. The membranes were then washed with the antibody dilution buffer for 30 min. They were then treated with the ECL-plus Western blotting detection system (Amersham Biosciences) after treatment with anti-rabbit or anti-mouse antibody (for analysis using Bid). They were then exposed to Hyperfilm™ ECL chemiluminescence film (Amersham Biosciences) at room temperature for 2 min. The chemiluminescent signals were visualized with a CS Analyzer and AE-6962 light capture (ATTO).

3. Results

3.1. *Morphology of the SDHC E69 cells on nude mouse*

It is known that NIH3T3 cells are transformed at high frequency by spontaneous mutations during long passage time or culture time. In fact, the cells, which did not proliferate within two weeks after the injection under the epithelium of nude mice (Figure 1A), grew into huge malignant tumors one month (Figure 1B). Some of the SDHC E69 cells that escaped from apoptosis underwent transformation, as evidenced by the fact that SDHC E69 transformed cells caused tumors within two weeks when injected under the epithelium of nude mice (Figure 1C) (*6*). The size of tumors remained unchanged even after one and a half month (Figure 1D). As expected of actively proliferating neoplasms, the tumors derived from the NIH3T3 cells had evidence of the apocytes and the nuclear divisions with characteristic dense staining of the cytoplasm (Figure 2A). In addition, the margin between the tumor and the blood vessel was distinct (Figure 2B). In contrast, The SDHC E69-derived tumors showed no evidence of nuclear divisions and showed nuclear aggregation (Figure 2C). They had assumed the posture of a fibrous tumor, and the blood vessel and tumor border was not distinct. Moreover, tumor-associated cells were present (Figure 2D). Thus, the thickness of the tumor cells layer was less when derived from SDHC E69 cells (Figure 2F) versus the wild type cells (Figure 2E).

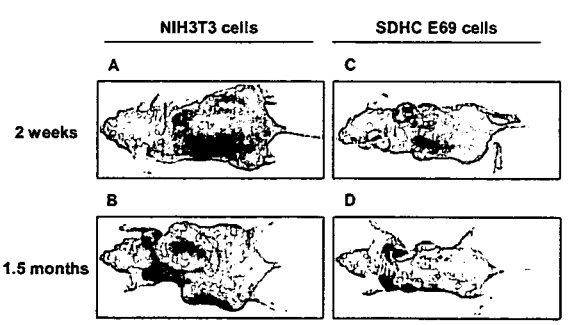

Figure 1. Comparisons of tumorigenesis using NIH3T3 cells and SDHC E69 cells injected into the epithelia of nude mice and cultured for two weeks and one and a half-months. Transplantation of spontaneous transformation NIH3T3 cells (A and B) and SDHC E69 cells (C and D) in epithelia of nude mice.

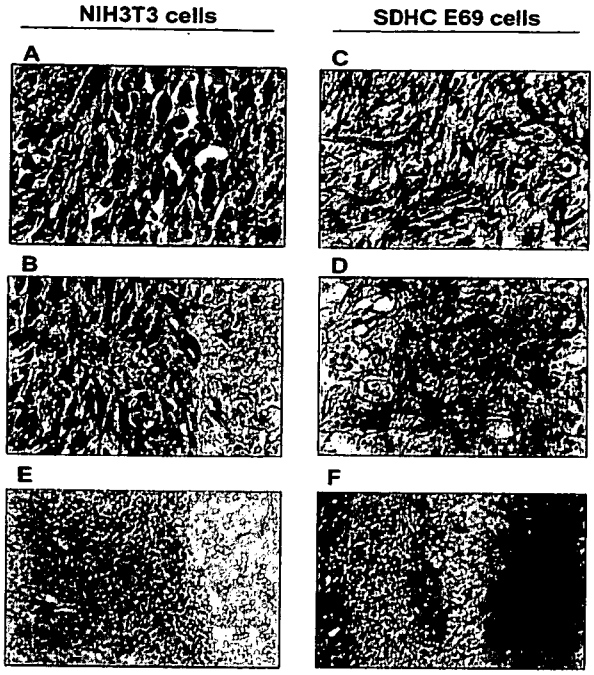

Figure 2. The tissue specimen of the tumor into epithelia of nude mice in spontaneous transformation NIH3T3 cells (A, B, E) and in SDHC E69 cells (C, D, F).

3.2. *The role of mitochondrial function to apoptosis*

Cellular cytochrome c was found in the mitochondria in both the SDHC E69 cells and NIH3T3 cells (Figure 3A). Cytosolic levels in the SDHC E69 cells and NIH3T3 cells were lower than mitochondrial levels. However, cytosolic cytochrome c levels increased significantly in the SDHC E69 cells.

In the mitochondria of the SDHC E69 cells compared to NIH3T3 cells, the Bax levels were significantly higher (Figure 3A). Bid and tBid levels were barely detectable in the SDHC E69 cells (Figure 3A).

In NIH3T3 cells, MDM2 mRNA expression was equally distributed between the 3.0 kbp and 1.7 kbp mRNAs, which are translated into the p90 and p76 MDM2 proteins, respectively (Figure 3B). A dramatically different pattern was observed in the SDHC E69 cells, as only the short-form type was expressed, which is incapable binding to and promoting p53 protein degradation (Figure 3B). p53 protein levels were below the level of detection in NIH3T3 cells (Figure 3C). Conversely, p53 protein existed in copious

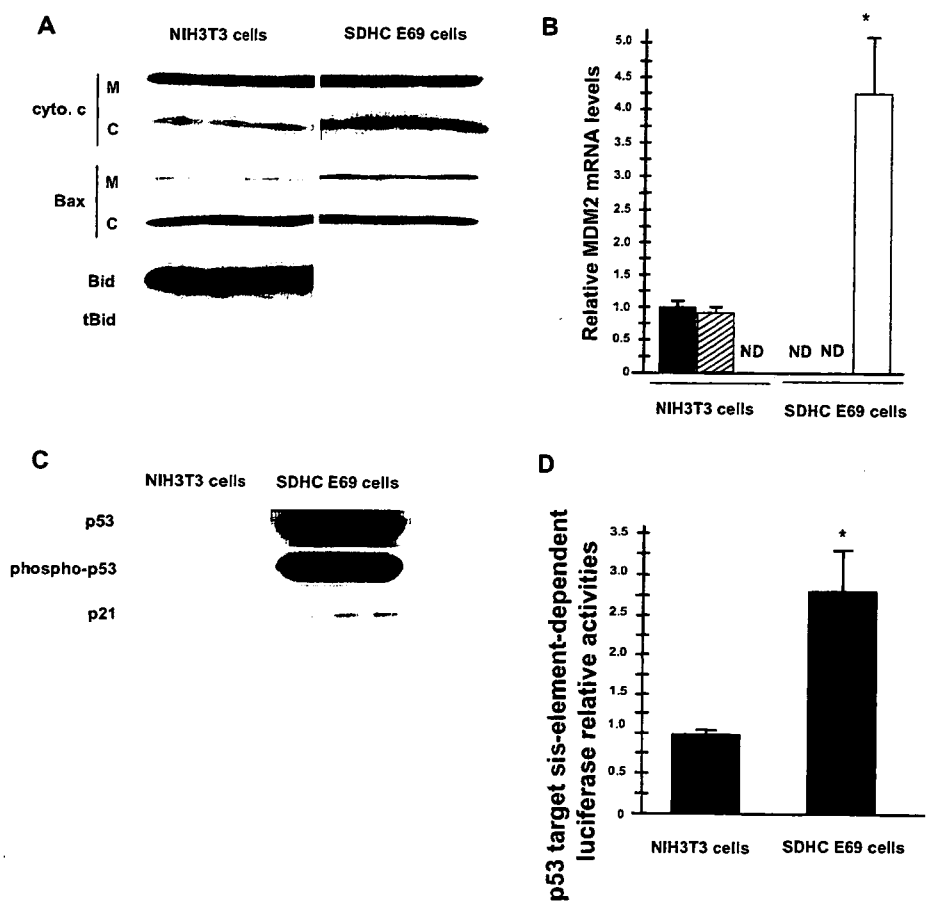

Figure 3. The alteration of cytochrome c release, inducible protein localization and p53 activation in NIH3T3 and SDHC E69 cells. A: Detection of cytochrome c, Bax and Bid proteins levels by Western blot analysis. cyto. c: cytochrome c, M: mitochondrial fraction, C: cytoplasmic fraction. $n = 3$. B: Detection of MDM2 mRNA patterns and expression levels by Northern blot analysis. MDM2 mRNA patterns of 3.0 kbp (p90, full-length MDM2) (closed boxes), 1.7 kbp (p76, not containing p53 binding motif) (hatched boxes) and 1.0 kbp (short form, not containing proteins binding motif) (open boxes) were detected. * $p < 0.01$, $n = 3$. C: Detection of p53, phospho-p53 and p21 protein levels by Western blot analysis. $n = 3$. D: Measurement of p53-dependent transcriptional activation levels by p53 target cis-element-dependent luciferase activity. * $p < 0.01$, $n = 3$.

amounts in the SDHC E69 cells, in which the short-form type MDM2 mRNA was expressed (Figure 3C). Moreover, most of the p53 protein was phosphorylated at serine residue 15 (Figure 3C). In addition, p21 protein was highly expressed in the SDHC E69 cells but not in NIH3T3 cells (Figure 3C). In the each cell lines transiently transfected a luciferase-containing construct with a p53 binding cis-elements, luciferase activity was over 2.8 times higher in the SDHC E69 cells than in the NIH3T3 cells (Figure 3D).

3.3. *The role of caspase 8 and caspase 9 on apoptosis*

As demonstrated previously, caspase 3 levels were higher in the SDHC E69 cells than in NIH3T3 cells (Figure 4A) (*6*). In the NIH3T3 cells, caspase 3 activity was slightly decreased by each caspase antagonist ($p < 0.01$) (Figure 4A). Caspase 3 activity was not further reduced by addition of both caspase 8 and 9 antagonists in the NIH3T3 cells (Figure 4A). In the SDHC E69 cells, both caspase 8 and caspase 9 inhibition had a larger effect on caspase 3 activity (Figure 4A). Moreover, we tested the viability of cells cultured in the presence of each caspase antagonist. The survival rate of the NIH3T3 cells was decreased by treatment with a caspase 9 antagonist (Figure 4B).

In contrast to the results obtained with NIH3T3 cells, the presence of each caspase antagonist resulted in increased the cell growth and proliferation in the SDHC E69 cells (Figure 4C). Moreover, both caspase 8 and 9 antagonists were inadequate to substantially reduce caspase 3 activity in the SDHC E69 cells ($p < 0.01$) (Figure 4A).

3.4. *The role of transduction pathway to apoptosis and tumorigenesis*

First, we analyzed p21Ras (H-, N-, K-Ras) and M-Ras mRNA expression levels by Northern blot analysis. Relative to the actin and G3PDH internal controls, p21Ras and M-Ras mRNA expression levels in the SDHC E69 cells were increased in comparison with the NIH3T3 cells (Figure 5A).

Relative to the actin and G3PDH internal standards, Raf-1/C-Raf mRNA expression, which induces cell growth and proliferation, was significantly increased in the SDHC cells in comparison to the NIH3T3 cells (Figure 5B). 195 kDa full-length MEKK1 protein was present in unchanged amount in the SDHC E69 cells, but the activated p91kDa MEKK1 protein was increased (Figure 5C). In addition, activated 54 kDa and 46 kDa JNK proteins were present in increased amounts in the SDHC E69 cells (Figure 5C). Conversely, the accumulation of activated p38 MAPK protein was not altered (Figure 5C). An AP-1 cis-element-dependent luciferase assay showed that JNK-dependent transcription was activated in the SDHC E69 cells (Figure 5D).

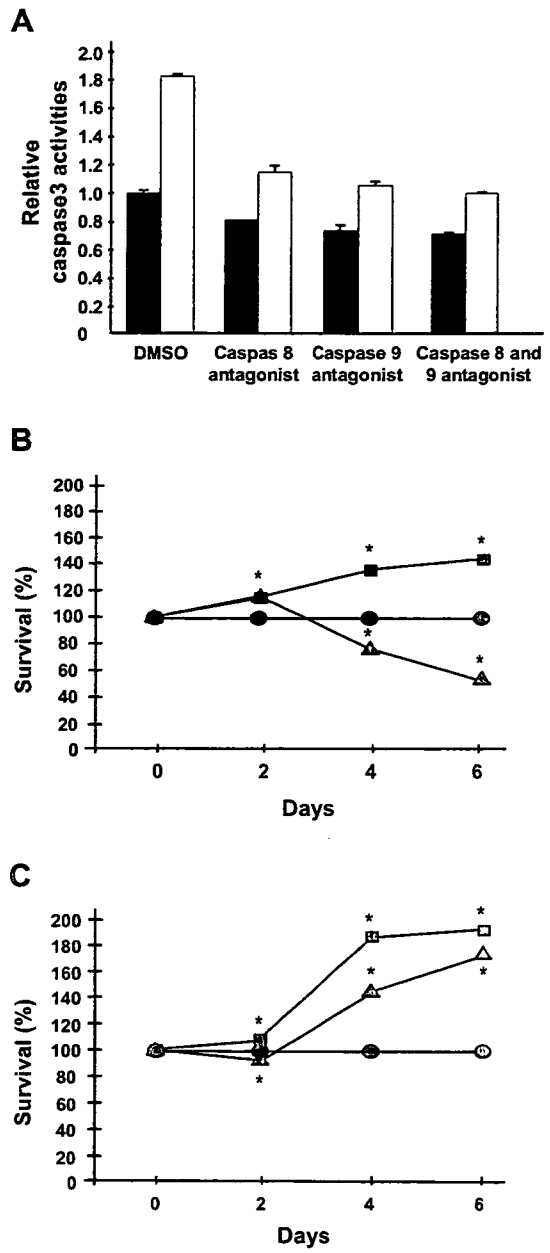

Figure 4. Variation of caspase 3 activity and survival rate by in response to caspase 8 and 9 antagonists. A: Caspase 3 levels were measured in NIH3T3 cells cultured for 3 month (closed boxes) and SDHC E69 cells (open boxes) in the presence of caspase 8 and 9 antogonists. $n = 3$. B and C: Viability of NIH3T3 cells (B), SDHC E69 cells (C) grown in the presence of caspase 8 (■) and caspase 9 (▲) antagonists and DMSO (●) additions. * $p < 0.01$, $n = 3$.

4. Discussion

We have previously established a transgenic SDHC E69 mouse cell line that contains a mutated SDHC subunit in complex II of the electron transport system (*6*). The SDHC E69 cells overproduced superoxide anion from mitochondria had elevated cytoplasmic carbonyl proteins and 8-OHdG in their DNA as well

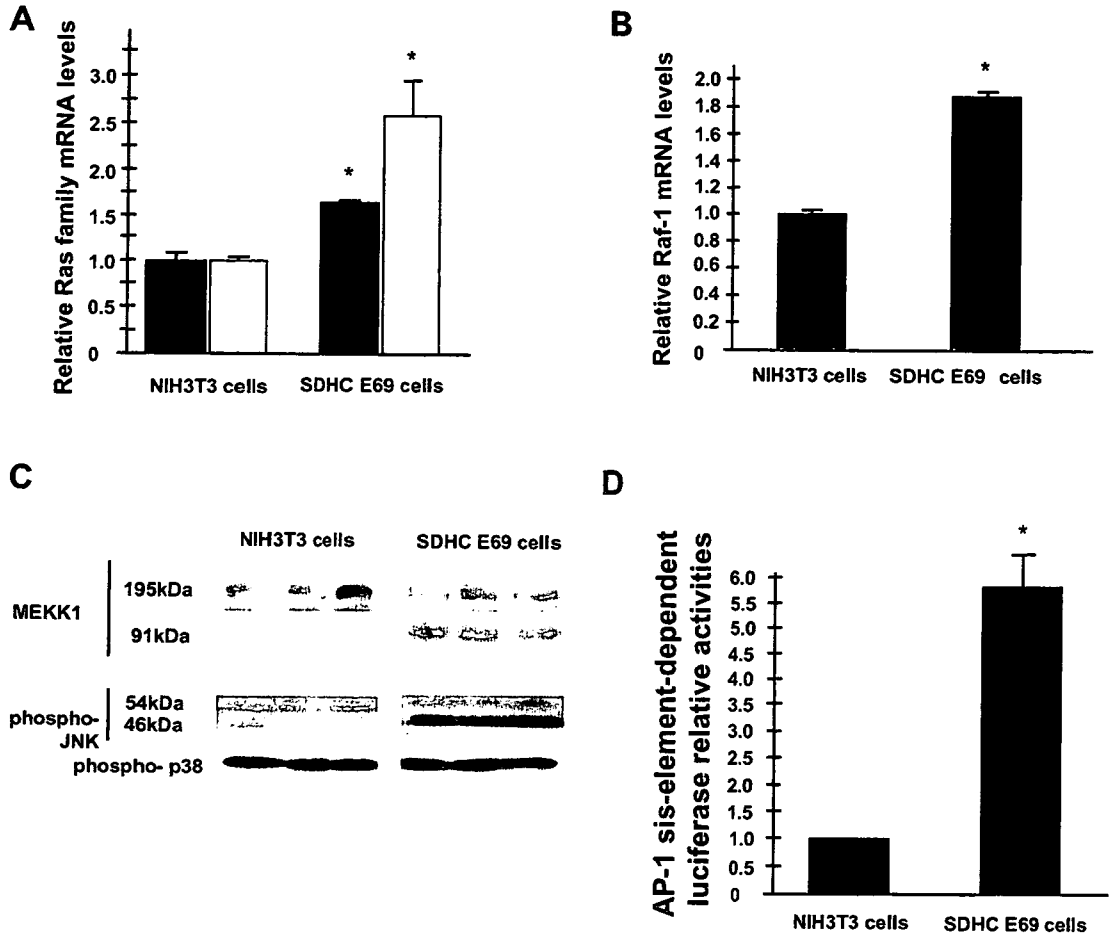

Figure 5. Alteration of stress-induced Ras-Raf and Ras-MEKK signal transduction pathways. A and B: Measurement of p21Ras (H-, N-, K-) (closed boxes), M-Ras (open boxes) (A) and Raf-1 mRNA expression levels (B) by Northern blot analysis. * $p < 0.01$, $n = 3$. C: Detection of MEKK1, phosphorylated JNK and p38 MAPK proteins, which are located and activated in downstream of MEKK1 activation, by Western blot analysis. $n = 3$. D: Measurement of transcriptional activation dependent on JNK activity by AP-1 cis-element-dependent luciferase activity. * $p < 0.01$, $n = 3$.

as significantly higher mutation frequencies than wild type (NIH3T3). There were many apoptotic cells in this cell line, as predicted by the observed increase in caspase 3 activity, decrease in mitochondrial membrane potential and structural changes in their mitochondria (*6*). In addition, some cells that escaped from apoptosis underwent transformation, as evidenced by the fact that SDHC E69 cells caused tumors within two weeks when injected under the epithelium of nude mice (Figure 1C) (*6*). The size of tumors remained unchanged even after one month (Figure 1D). It is known that NIH3T3 cells are transformed at high frequency by spontaneous mutations during long passage time or culture time. In fact, the cells, which did not proliferate within two weeks after the injection under the epithelium of nude mice, grew into huge malignant tumors one month (Figure 1A and B).

The SDHC E69-derived tumors showed no evidence of nuclear divisions and showed nuclear aggregation (Figure 2C). They had assumed the posture of a fibrous tumor, and the blood vessel and tumor border was not distinct. Moreover, tumor-associated cells were present (Figure 2D). In contrast, as expected of actively proliferating neoplasms, the tumors derived from the NIH3T3 cells had evidence of the apocytes and the nuclear divisions with characteristic dense staining of the cytoplasm (Figure 2A). In addition, the margin between the tumor and the blood vessel was distinct (Figure 2B). Thus, the thickness of the tumor cells layer was less when derived from SDHC E69 cells versus the NIH3T3 cells (Figures 2E and F). These histological data are consistent with the notion that the NIH3T3 cells are actively proliferating while the SDHC E69 cells are not. We speculate that there was no increase in overall tumor mass because cell proliferation was counterbalanced by increased levels of apoptosis.

Mitochondria from SDHC E69 cells overproduced O_2^-, leading to wide-spread apoptosis as caspase 3 levels were elevated (*6*). Caspase 3 acts relatively late in the caspase cascade, after cells are inextricably committed to apoptosis. To elucidate the mechanisms by which overproduction of O_2^- leads to supernumerary apoptosis, we examined the activities of various components of the apoptotic machinery as well as the various signaling

pathways that promote apoptosis. We first examined cytosolic and mitochondrial levels of cytochrome c in the SDHC E69 cells after the establishment and their NIH3T3 progenitors. Cytochrome c is known to be released from mitochondria and combines with apoptosis protease activating factor-1 (Apaf-1), procaspase 9, and dATP in the cytosol, triggering the activation of caspase 3 (*9*). As expected given its role in electron transport, cellular cytochrome c was found in the mitochondria in both the SDHC E69 cells and NIH3T3 cells (Figure 3A). Cytosolic levels in the SDHC E69 cells and NIH3T3 cells were lower than mitochondrial levels. However, cytosolic cytochrome c levels increased significantly in the SDHC E69 cells. This is consistent with the increase in caspase 3 that we have documented previously (*9*) and suggests strongly that elevated O_2^- production in the SDHC E69 cells sets into motion events that enable cytochrome c leakage from mitochondria, with caspase 3 activation and apoptosis the downstream consequences. We then examined the status of two proapoptotic members of the Bcl-2 family. First, we looked at Bax, which regulates cytochrome c release from mitochondria by translocating from the cytoplasm to mitochondria and subsequently altering mitochondrial membrane permeability (*10*). Bax primarily localized to the cytosol. In the mitochondria of the SDHC E69 cells compared to NIH3T3 cells, the Bax levels were significantly higher (Figure 3A). These results suggest that the increased cytosolic cytochrome c levels observed in the SDHC E69 cells could be attributed at least in part to Bax translocation. Second, we analyzed the Bid protein, which is activated by caspase 8 cleavage to produce 15 kDa tBid. tBid translocates to mitochondria to facilitate cytochrome c release by interacting with Bax (*11*). Bid and tBid levels were barely detectable in the SDHC E69 cells (Figure 3A). These results suggest that cytochrome c release was mainly caused by Bax localized in mitochondria. We also examined the activation of the tumor suppressor gene p53, as p53 has long been known to act as a transcription factor to promote apoptosis via Bax action (*12*). More recently, p53 has been also been shown to localize to mitochondria and, in a transcription-independent fashion, play an important role in the mitochondrial apoptotic pathway (*13*). We asked whether p53 might be involved in the cellular responses to the oxidative stress inherent to the SDHC E69 cells. Since p53 levels are normally held low via the action of MDM2, we examined MDM2 mRNA expression using Northern blot analyses. MDM2 mRNA exists in three isoforms: 3.0 kbp, 1.7 kbp and several short-forms (of roughly 1.2 kbp) which are generated by alternative splicing. They are translated into several forms, including p90 (which possesses p53 binding capacity), p76 (which lacks p53 binding ability) and short-form types (which also lack p53 activity and are found in transformed cells) (*14*). In NIH3T3 cells, MDM2 mRNA expression was equally distributed between the 3.0 kbp and 1.7 kbp mRNAs, which are translated into the p90 and p76 MDM2 proteins, respectively (Figure 3B). A dramatically different pattern was observed in the SDHC E69 cells, as only the short-form type was expressed, which is incapable binding to and promoting p53 protein degradation (Figure 3B). These results led us to test p53 protein levels by Western blot analysis. p53 levels were below the level of detection in NIH3T3 cells (Figure 3C). Conversely, p53 protein existed in copious amounts in the SDHC E69 cells, in which the short-form type MDM2 mRNA was expressed (Figure 3C). Moreover, most of the p53 protein was phosphorylated at serine residue 15 (Figure 3C), a modification known to activate p53 as a transcription factor, leading to cell-cycle arrest and apoptosis (*15*). These results strongly suggest that p53 exists as an active transcription factor in the SDHC E69 cells. We confirmed this in two ways. First, p21 protein, which is a p53 target gene and promotes the cell-cycle arrest, was highly expressed in the SDHC E69 cells but not in NIH3T3 cells (Figure 3C). Second, a luciferase-containing construct with a p53 binding cis-elements was transiently transfected into the each cell lines. Luciferase activity was over 2.8 times higher in the SDHC E69 cells than in the NIH3T3 cells (Figure 3D). Collectively, these data show that in the SDHC E69 cells, the oxidative stress resulting from mitochondrial overproduction of O_2^- leads to altered mRNA expression of MDM2 which in turn results in p53 accumulation and activation. As a consequence, p21 and presumably other p53 target genes are induced, resulting in cell-cycle delays and apoptosis. It is also possible that p53 is present in the mitochondria of the SDHC E69 cells to promote cytochrome c release and trigger apoptosis.

We next analyzed the relative roles played by caspase 8 and caspase 9 in elevated apoptosis in the SDHC E69 cells. Caspase 8 acts as an initiator caspase in the extrinsic apoptotic pathway while caspase 9 is activated by cytochrome c to initiate the intrinsic (mitochondrial) apoptotic pathway (*9*). When cleaved, both proteolytically activate executioner caspases such as caspase 3. We employed caspase 8 and 9 antagonists for this purpose and measured caspase 3 activity. As demonstrated previously, caspase 3 levels were higher in the SDHC E69 cells than in NIH3T3 cells (Figure 4A). In the NIH3T3 cells, caspase 3 activity was slightly decreased by each caspase antagonist ($p < 0.01$) (Figure 4A). Caspase 3 activity was not further reduced by addition of both caspase 8 and 9 antagonists in the NIH3T3 cells (Figure 4A). Since both caspase 8 and 9 participate in the extrinsic pathway, these results suggest that both caspases are active in NIH3T3 cells, albeit at low levels, in response to the low levels of extrinsic oxidative stress normally present in cultured cells. In the SDHC E69 cells, both

caspase 8 and caspase 9 inhibition had a larger effect on caspase 3 activity (Figure 4A). Since caspase 9 acts downstream of mitochondria, this suggests that the elevated apoptosis in the SDHC E69 transformed cells was the result of increased ROS generation in their mitochondria rather than involving the extrinsic pathway, in which case both caspase antagonists would be expected to have roughly equal inhibitory effects. Moreover, we tested the viability of cells cultured in the presence of each caspase antagonist. The survival rate of the NIH3T3 cells was decreased by treatment with a caspase 9 antagonist (Figure 4B). Some necrotic cell death was observed under these conditions (data not shown). Given that necrotic cell deaths were rarely observed in cells not treated with the caspase antagonists, we speculate that one consequence of the caspase 9-induced apoptosis is to protect tissues from stress-induced necrotic cell death that would otherwise result from mitochondrial oxidative stress.

In contrast to the results obtained with NIH3T3 cells, the presence of each caspase antagonist resulted in increased the cell growth and proliferation in the SDHC E69 cells (Figure 4C). This suggests that the SDHC E69 transformed cells might have developed oxidative stress resistance or even dependent cell growth and proliferation mechanisms. Moreover, both caspase 8 and 9 antagonists were inadequate to substantially reduce caspase 3 activity in the SDHC E69 cells ($p < 0.01$) (Figure 4A). This led us to speculate that a signal transduction pathway might be operative in these cells. Thus, while cytochrome c release from mitochondria was an important intermediary participant, components upstream of the mitochondria and independent of the mitochondria were responsible for initiating the apoptotic process in the SDHC E69 cells.

The Ras-Raf and Ras-MEKK signal transduction pathway has been shown to promote apoptosis in a mitochondria-independent fashion (*16*). For example, MEKK1 can be cleaved by many stimuli to generate a 91 kDa kinase that is a strong inducer of apoptosis (*17,18*). We tested to see if some of the elevated apoptosis in the 3-month SDHC E69 cells might be due to the activation of such signal transduction pathways. First, we analyzed p21Ras (H-, N-, K-Ras) and M-Ras mRNA expression levels by Northern blot analysis. Relative to the actin and G3PDH internal controls, p21Ras and M-Ras mRNA expression levels in the SDHC E69 cells were increased in comparison with the NIH3T3 cells (Figure 5A). Second, we tested Raf-1/C-Raf mRNA expression and MEKK1 protein concentration by Northern and Western blot analyses. Relative to the actin and G3PDH internal standards, Raf-1/C-Raf mRNA expression, which induces cell growth and proliferation, was significantly increased in the SDHC E69 cells in comparison to the NIH3T3 cells (Figure 5B). In additional, 195 kDa full-length MEKK1 protein, which can be cleaved to activate caspase 3, was present in unchanged amount in the SDHC E69 cells, but the activated p91 kDa MEKK1 protein, which induces apoptosis independent of the mitochondrial pathway, was increased (Figure 5C). Thus, it appears that Ras acts to increase MEKK1 expression in response to the oxidative stress and MEKK1 has been cleaved into its active form in the SDHC E69 cells. In addition, we analyzed JNK and p38 MAPK, which are located further downstream in these signal transduction pathways. Activated 54 kDa and 46 kDa JNK proteins were present in increased amounts in the SDHC E69 cells (Figure 5C). Conversely, the accumulation of activated p38 MAPK protein was not altered (Figure 5C). We also performed an AP-1 cis-element-dependent luciferase assay, which serves as a measure of JNK activity. JNK-dependent transcription was activated in the SDHC E69 cells (Figuer 5D).

We speculate that this explains the phenotypes we have previously observed in the SDHC E69 cells; namely, those of increased apoptosis, high levels of transformation into neoplasms and hypermutability. In addition, the growth characteristics of SDHC E69 cells in the epithelium of nude mice appear to mimic the slow growth of PGLs. It has been reported that the hereditary PGLs that are usually characterized by the development of benign, neural-crest-derived, slow-growing tumors of parasympathetic ganglia which are caused by mutations in the SDHC gene. Between 10% and 50% of cases are familial and are transmitted in an autosomal dominant fashion with incomplete and age-dependent penetrance. We speculate that these characteristics are related to the apoptosis induction caused by the mitochondrial.

Acknowledgements

We are indebted Ms. H. Mitani and Y. Hirayama, Cancer Institute, Japanese Foundation for Cancer Research, for the work using Nude mice. This work is supported by grant-in-aid for Scientific Research from the Ministry of Education, Culture, Sports, Science and Technology and for Aging Research from the Ministry of Health, Labor and Welfare, Japan and the Takeda Science Foundation.

References

1. Turrens JF. Superoxide production by the mitochondrial respiratory chain. Biosci Rep 1997; 17:3-8.
2. Ishii N, Fujii M, Hartman PS, Tsuda M, Yasuda K, Senoo-Matsuda N, Yanase S, Ayusawa D, Suzuki K. A mutation in succinate dehydrogenase cytochrome b causes oxidative stress and aging in nematodes. Nature 1998; 394:694-697.
3. Senoo-Matsuda N, Yasuda K, Tsuda M, Ohkubo T, Yoshimura S, Nakazawa H, Hartman PS, Ishii N. A defect in the cytochrome b large subunit in complex II causes both superoxide anion overproduction and

abnormal energy metabolism in Caenorhabditis elegans. J Biol Chem 2001; 276:41553-41558.
4. Senoo-Matsuda N, Hartman PS, Akatsuka A, Yoshimura S, Ishii N. A complex II defect affects mitochondrial structure, leading to ced-3 and ced-4-dependent apoptosis and aging. J Biol Chem 2003; 278:22031-22036.
5. Hartman PS, Ponder R, Lo HH, Ishii N. Mitochondrial oxidative stress can lead to nuclear mutability. Mech Ageing Develop 2004; 125:417-420.
6. Ishii T, Yasuda K, Akatsuka A, Hino O, Hartman PS, Ishii N. A mutation in the SDHC gene of complex II increases oxidative stress, resulting in apoptosis and tumorigenesis. Cancer Res 2005; 65:203-209.
7. Niemann S, Muller U. Mutations in SDHC cause autosomal dominant paraganmlioma, type 3. Nat Genet 2000; 26:268-270.
8. Baysal BE, Ferrell RE, Willett-Brozick JE, Lawrence EC, Myssiorek D, Bosch A, van der Mey A, Taschner PE, Rubinstein WS, Myers EN, Richard CW 3rd, Cornelisse CJ, Devilee P, Devlin B. Mutations in SDHD, a mitochondrial complex II Gene, in hereditary paraganglioma. Science 2000; 287:848-851.
9. Budihardjo I, Oliver H, Lutter M, Luo X, Wang X. Biochemical pathways of caspase activation during apoptosis. Annu Rev Cell Dev Biol 1999; 15:269-290.
10. Jürgensmeier JM, Xie Z, Deveraux Q, Ellerby L, Bredesen D, Reed JC. Bax directly induces release of cytochrome c from isolated mitochondria. Proc Natl Acad Sci USA 1998; 95:4997-5002.
11. Luo X, Budihardjo I, Zou H, Slaughter C, Wang X. Bid, a Bcl2 interacting protein, mediates cytochrome c release from mitochondria in response to activation of cell surface death receptors. Cell 1998; 94:481-490.
12. Shen Y, White E. p53-dependent apoptosis pathways. Adv Cancer Res 2001; 82:55-84.
13. Mihara M, Erster S, Zaika A, Petrenko O, Chittenden T, Pancoska P, Moll UM. p53 has a direct apoptogenic role at the mitochondria. Mol Cell 2003; 11:577-590.
14. Sigalas I, Calvert AH, Anderson JJ, Neal DE, Lunec J. Alternatively spliced mdm2 transcripts with loss of p53 binding domain sequences: transforming ability and frequent detection in human cancer. Nat Med 1996; 2:912-917.
15. Shieh SY, Ikeda M, Taya Y, Prives C. DNA damage-induced phosphorylation of p53 alleviates inhibition by MDM2. Cell 1997; 91:325-334.
16. Russell M, Lange-Carter CA, Johnson GL. Direct interaction between Ras and the kinase domain of mitogen-activated protein kinase kinase kinase (MEKK1). J Biol Chem 1995; 270:11757-11760.
17. Widmann C, Gerwins P, Johnson NL, Jarpe MB, Johnson GL. MEK kinase 1, a substrate for DEVD-directed caspases, is involved in genotoxin-induced apoptosis. Mol Cell Biol 1998; 18:2416-2429.
18. Gibson EM, Henson ES, Villanueva J, Gibson SB. MEK kinase 1 induces mitochondrial permeability transition leading to apoptosis independent of cytochrome C release. J Biol Chem 2002; 277:10573-10580.

(Received December 14, 2007; Revised January 22, 2008; Accepted January 25, 2008)

ORIGINAL ARTICLE

A low cost and quick assay system using the free-living nematode *Caenorhabditis elegans* to determine the effects of Kampo medicines on life span

Takuro Yamaguchi[1, 2], Akira Onodera[1], Kayo Yasuda[3], Yasunori Nishio[2, 4], Makoto Arai[5], Michio Tsuda[1], Masaki Miyazawa[1], Philip S. Hartman[6] and Naoaki Ishii[1, 2]

[1] *Department of Molecular Life Science, Tokai University School of Medicine, Japan*
[2] *NemaBio, Inc., Japan*
[3] *Teaching and Research Support Center, Tokai University School of Medicine, Japan*
[4] *Towa Scientific Co., LTD, Japan*
[5] *Department of Oriental Medicine, Tokai University School of Medicine, Japan*
[6] *Biology Department, Texas Christian University, USA.*

Abstract
A low cost and quick assay system has been developed using the free-living nematode *Caenorhabditis elegans* to determine the effects of Kampo medicines (traditional Japanese medicines) on life span. A key characteristic of this system is the use of a *fer-15* mutant, which is sterile when grown at 25°C owing to the production of spermatids that fail to activate into spermatozoa. This prevented the production of progeny, which would otherwise complicate life span analyses. In addition, liquid culture medium permitted easy handling of the test subjects. We employed this system to examine the longevity effects of 26 Kampo medicines and crude drugs. Of these, *Rhei Rhizoma* was found to extend the life span and acts as an anti-oxidant that suppresses superoxide anion generation from mitochondria.

Key words: *C. elegans; life span; Kampo medicines; crude drugs; oxidative stress*

Introduction

A number of assay systems have been developed to screen chemicals for their ability to confer favorable phenotypes. Most of these systems are *in vitro* or *in vivo* using single-cell organisms or cells in tissue culture, whereas systems using multi-cellular organism are few owing to both labor and cost intensity. We now report of a low cost and rapid assay system at the whole-animal level that we employed to find natural endowments or chemicals with longevity effects in the free-living nematode *Caenorhabditis elegans* (*C. elegans*). *C. elegans* offers several distinct advantages for aging research at the organismal level (Luo, 2006), not the least of which is a short maximum life span of approximately 30 days (Klass and Hirsh, 1976; Honda *et al.*, 1993)(Fig. 1). Its soma consists of fewer than 1,000 cells including hypodermis, digestive organ, neurons, musculature, and reproductive organs (Sulston and Horvitz, 1977). All of

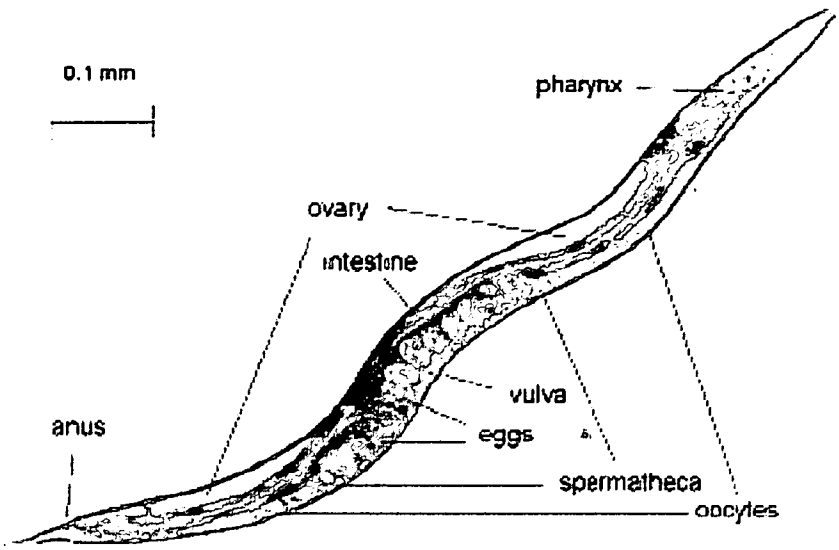

Fig.1 Photomicrograph showing major anatomical features of a *C. elegans* adult hermaphrodite.

these are postmitotic in adults, thus offering the opportunity to detect cumulative age-related cellular alterations (Hosokawa *et al*, 1994; Adachi *et al*., 1998; Ishii *et al*, 2002). Embryonic development is rapid, taking only 13 h at 20°C (Sulston, 1988; Wood, 1988). After hatching, larval development proceeds through four molts, which punctuate larval stages L1 through L4. Animals reproduce with a rapid life cycle of approximately 3.5 days at 20°C. *C. elegans* also offer an advantage to screen drugs that may increase life span because they live only for 30 days (Melov *et al*, 2000; Ishii *et al*, 2004; Petrascheck *et al*, 2007). In general, *C. elegans* can be readily cultured on agar plate in petri plates on a simple diet of *Escherichia coli* (*E. coli*) (Brenner, 1974). They also can be grown in liquid culture in the presence or absence of bacteria (Vanfleteren, 1980; Jansson *et al*, 1986; Jewitt *at al*, 1999; Houthoofd *et al*, 2002). Liquid culture system is convenient to treat many animals and permitted easy handling of the test subjects rather than agar plate, but animals do not grow well in liquid culture compared to agar plate and seem not to be health because of poor diet. It is known that the life span of *C. elegans* is dependent on the concentration of *E. coli* which often serves as its food (Klass, 1977). In our liquid culture system, Bacto-peptone as nutrition for *E. coli* was increased so that this defect was overcome.

C. elegans normally reproduces as a bisexual hermaphrodite that produces both oocytes and sperm. Animals normally reproduce by self-fertilization. In order to prevent the progeny production, 5-fluoro-2-deoxyuridine (FudR) has generally been used after maturation (Mitchell *et at*., 1979). In our system, we used *fer-15* mutant, which when grown at 25°C produces spermatids that fail to activate into spermatozoa (Roberts and Ward, 1982). In this report, we introduce a low cost and rapid assay system that examines the life span of a *fer-15* mutant as a marker for the isolation of Kamopo medicines and crude drugs with macrobiotic activity.

Kamopo medicines (traditional Japanese medicines) and crude drugs are known to have many biological effects. In part owing to the current fitness fad in the world, researchers have attempted to identify chemicals that promote longevity and good health (Kishikawa, *et al*., 1997). We employed this system to examine 26 Kamopo medicines and crude drugs. Of these samples, *Rhei Rhizoma* was found to extend the life span.

Recently, much attention has been focused on the hypothesis that oxidative damage plays a major role in cellular and organismal aging (Finkel and Holbrook, 2000). There are many reports that anti-oxidant agents and enzymes extend life span of several animals, including *C. elegans* (Haenold

et al., 2005). It is known that oxygen is initially converted to superoxide anion (O_2^-), one of several reactive oxygen species (ROS), by electron leakage. This occurs primarily from complex III of the electron transport system present in mitochondria and constitutes the major endogenous source of ROS (Turrens *et al.*, 1985; Lenaz, 1998; Finkel and Holbrook, 2000; Raha, and Robinson, 2000). Such endogenously generated ROS readily attack a wide variety of cellular entities, resulting in damage that compromises cell integrity and function (Vuillaume, 1987; Collins *et al*, 1997). We found that the *Rhei Rhizoma* has a role of anti-oxidant, which suppress O_2^- generation from mitochondria and extends the life span of *C. elegans*.

Materials and Methods

1. Materials

C. elegans, wild-type and a *fer-15* (*hc15*) mutant strain were obtained from the Caenorhabditis Genetics Center, University of Minnesota. Animals were cultured on nematode growth medium (NGM) agar plates seeded with the *Escherichia coli* (*E. coli*) strain OP50 at 20°C as previously described (Brenner, 1974). Embryos (eggs) were collected from young adult hermaphrodite on NGM agar plates using alkaline sodium hypochlorite (Emmons *et al.*, 1979). The released eggs were allowed to hatch by overnight incubation at 20°C in S basal buffer [100 mM NaCl, 50 mM potassium phosphate (pH 6.0)] (Sulston and Brenner, 1974).

Kampo medicines: *daisaikoto, shosaikoto, saikokeishito, orengedokuto, tokishakuyakusan, keishibukuryogan, shigyakusan, hochuekkito, rikkunshito, shichimotsukokato, chotosan, juzentaihoto, seihaito, daikenchuto, goshajinkigan, saireito.*

Crude drugs: *Paeoniae Radix, Cinnamomi Cortex, Moutan Cortex, Glycyrrhizae Radix, Ginseng Radix, Zingiberis Rhizoma, Bupleuri Radix, Scutellariae Radix, Rhei Rhizoma, Ephedrae Herba.*

These Kampo medicines and crude drugs were kindly provided by the Tsumura Company.

2. Measurement of life span

NGM agar medium plates seeded with the *E. coli* strain OP50 as already described (Honda *et al.*, 1993; Adachi *et al.*, 1998; Ishii *et al.*, 1998) were used for both growth and determination of the life spans of wild-type and *fer-15* mutant hermaphrodites. 5-fluoro-2'-deoxyuridine (FudR) has been used after maturation in order to prevent the progeny production of wild type on NGM agar plate (Mitchell *et at.*, 1979). S medium (Sulston and Brenner, 1974) containing Bacto-peptone of various concentrations (a standard concentration was 2.5 g Bacto-peptone in 1,000 ml of the medium: x1) seeded with the *E. coli* strain OP50 was used to determine the life spans of the *fer-15* mutant in liquid medium. *E. coli* strain OP50 was cultured in 500 ml of LB medium [10 g Bacto-tryptone, 5 g yeast extract, 10 g NaCl, pH 7.0] at 37°C over night. After centrifugation at 3,000 rpm for 15 min, the pellet was suspended in 500 ml of the S medium. About 2,000 newly hatched larvae (L1-stage larvae) were added in 10 ml of the S medium into a 50 ml conical flask and incubated at 25°C for 100 rpm in a shaker (ISF-1-W, Kühner SHAKER, Switzerland). It was possible that some test samples inhibited *E. coli* growth, thereby affecting *C. elegans* life spans. In order to avoid this, a final concentration of 200 μg/ml of ampicillin was added in the S medium after animals reached to adulthood (4 days after the L1 stage-larvae were added in the S medium) in order to inhibit the *E. coli* proliferation. To measure life span, the numbers of living and dead animals in 300 μl of the medium in each flask were counted every few days.

3. Measurement of body size

Body length and width of animals from L1 stage to adult stage were measured daily during the six days after hatching.

4. Isolation of mitochondria

L4-stage wild-type animals were employed for mitochondrial isolation. A flotation method was used to remove debris and dead animals from living animals (Lewis *et al*, 1995). In brief, NGM agar plates were washed and the contents were suspended in ice-cold S basal buffer and mixed with an equal volume of ice-cold 60% sucrose. After centrifugation for 15 second at 3,000 rpm, the floating animals were transferred to a fresh tube. They were washed three times with S basal buffer and once with isolation buffer (210 mM mannitol, 70 mM sucrose, 0.1 mM EDTA and 5 mM Tris-HCl, pH 7.4). The animals were homogenized in isolation buffer using a teflon homogenizer. The debris was removed by a differential centrifugation at 600 x *g*. The supernatant was then centrifuged at 7,200 x *g* and the mitochon-

dria-containing pellet was suspended in TE buffer [50 mM Tris-HCl (pH 7.4), 0.1 mM EDTA]. Sub-mitochondrial particles (SMP) were employed in these experiments because they are known to be depleted in the mitochondrial superoxide dismutase that transforms superoxide anion to hydrogen peroxide. SMP were obtained by sonicating freeze-thawed mitochondria twice for 20 s separated by 1 min intervals in a model U200S sonicator (IKA Labortechnik). SMP were washed twice at isolation buffer and suspend in TE buffer.

5. Measurement of superoxide anion (O_2^-)

O_2^- production was measured using the chemiluminescent probe MPEC (2-methyl-6-p-methoxyphenylethynyl-imidazopyrazinone) (ATTO Co., Tokyo, Japan)(Shimomura *et al.*, 1998; Yasuda *et al.*, 2006). MPEC has an advantage of low background relative to MCLA (3,7-dihydro-2-methyl-6- (4-methoxyphenol) imidazol [1,2-a]pyrazin-3-one) that is generally used. 5 μg of SMP was added to 1 ml of assay buffer (50 mM HEPES-NaOH, pH 7.4, 2 mM EDTA) containing 0.7 μM MPEC. 5 μg/ml of *Rhei Rhizoma* was added in the SMP solution, which was placed into a photon counter with an AB-2200 type Luminescencer-PSN (ATTO Co., Tokyo, Japan) and measured at 37°C. The rates of O_2^- were expressed as counts per second.

6. Statistical analysis

Statistical analysis was carried out by Student's *t* test and Tukey's multiple-range test.

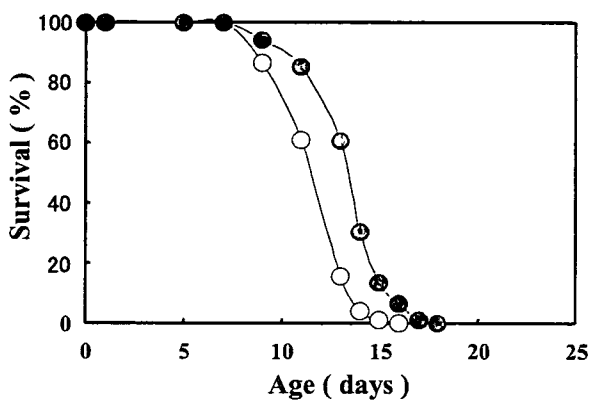

Fig. 2. Life spans of wild type N2 (closed circles) and a *fer-15* mutant (open circles) grown on NGM agar plates. 100 animals were measured for each strain at 25°C.

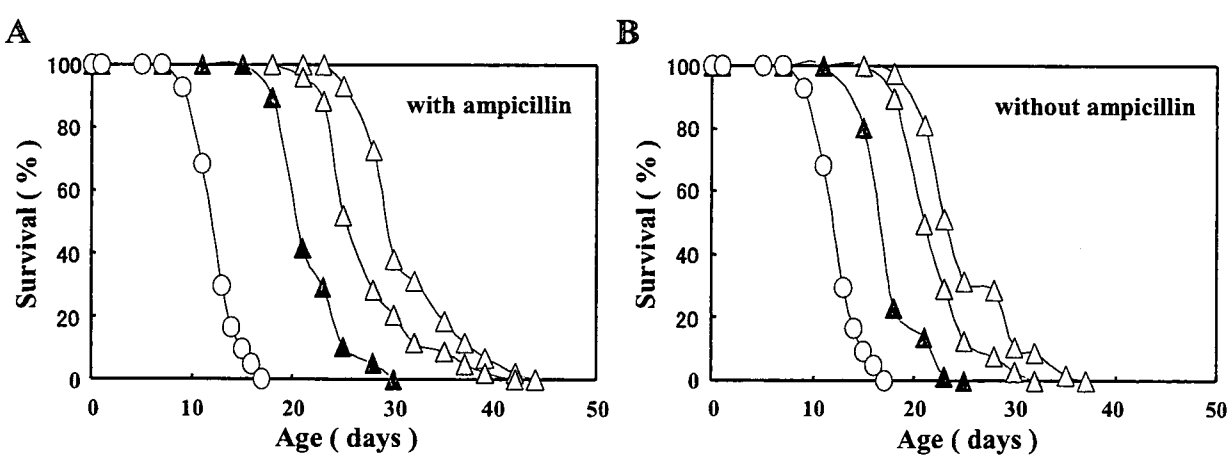

Fig. 3. Life spans of a *fer-15* mutant grown on NGM agar plate and in S medium containing various concentrations of Bacto-peptone with (A) and without ampicillin (B). Open circles: on NGM agar plates; open triangles: with a standard concentration of Bacto-peptone in liquid medium; ashen triangle: two-fold Bacto-peptone; closed triangles, four-fold Bacto-peptone. 100 animals were measured from the NGM agar plates. See also Table 1.

Results and Discussion

1. Development of the system

To develop a low cost and quick assay system using the free-living nematode, *Caenorhabditis elegans* (*C. elegans*) for identifying Kampo medicines and crude drugs with macrobiotic activity, a suitable assay was designed and tested. The life span of a *fer-15* mutant was slightly shorter than the wild type N2 on NGM agar plate (Fig. 2). The life spans decreased depending on the concentration of Bacto-peptone in the S medium (Fig. 3A; Table 1). The presence of ampicillin contributed to extend life span (Fig. 3B; Table 1), suggesting that caloric restriction to adult animals resulted in the extension of life span. Concentrations of Bacto-peptone in the S medium contributed markedly to body width but slightly to body length (Fig. 4A and 4B; Table 2A and 2B), suggested that the diet from *E. coli* affected to life span and body size. A four-fold concentration of Bacto-peptone in S medium gave the same body size of *C. elegans* adults as those grown on NGM agar plats (Fig. 4A and 4B; Table 2A and 2B.). In even Bacto-peptone of the standard concentration in S medium, animals appeared to be healthy.

In recent years, anti-aging studies for our health and longevity have been the subject of intense interest and experimentation. Physiologically functional nutrition as well as basic nutrition are especially studied. Our system has the potential to assist in identifying undiscovered natural endowments or chemicals with macrobiotic activities. We provide an example of this below.

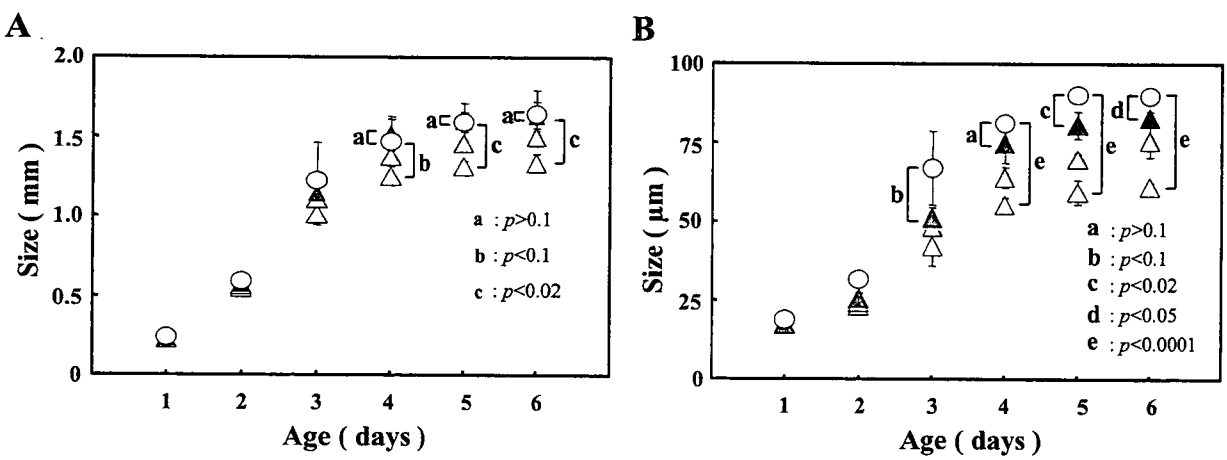

Fig. 4. Mean body length (A) and width (B) at different days of development. Open circles: on NGM agar plate; open triangles: with a standard concentration of Bacto-peptone in S medium; ashen triangles: two-fold Bacto-peptone; closed triangles, four-fold Bacto-peptone. Each symbol with error bars indicates the mean values with the standard deviations from three separate experiments. 25 animals were measured at each point in each experiment. See also Table 2.

Table 1. Life spans (mean and maximum life spans ± standard deviation) of the *fer-15* mutant grown on NGM agar plates and in S medium containing various concentrations of Bacto-peptone with and without ampicillin. Each value indicates the mean of three separate experiments.

Concentrations of Bacto-Peptone in S medium	Ampicillin	Life span (days)	
		Mean life span	Maximum life span
x 1	+	30.5 ± 2.02	40.3 ± 4.04
x 1	-	24.1 ± 2.77	32.7± 5.14
x 2	+	26.9 ± 1.62	36.7± 5.03
x 2	-	21.7 ± 2.48	29.7± 4.04
x 4	+	21.1 ± 1.93	27.7± 2.52
x 4	-	17.4 ± 1.62	22.7± 2.52
On NGM medium	-	12.5 ± 0.31	16.3 ± 0.58

2. *The longevity effects of Kampo medicines and crude drugs*

As a preliminary study, the life spans of the 16 Kampo medicines and 10 crude drugs were examined in S medium containing Bacto-peptone of a standard concentration and ampicillin. In these medicines and drugs, 8 different Kampo medicines (*daisaikoto*, *syosaikoto*, *saikokeishito*, *tokishakuyakusan*, *keishibukuryogan*, *shigyakusan*, *shichimotsukokato* and *daikenchuto*) and 3 crude drugs (*Moutan Cortex*, *Ginseng Radix* and *Bupleuri Radix*) had no effect on *C. elegans* life span in the S medium even at high concentrations (Fig. 5A, Table 3A and 3B). Figure 5A showed the result of *saikokeishito* as an example of this. On the other hand, 6 Kampo medicines (*orengedokuto*, *hochuekkito*, *rikkunshito*, *juzentaihoto*, *seihaito*, and *saireito*) and 6 crude drugs (*Paeoniae Radix*, *Cinnamomi Cortex*, *Glycyrrhizae Radix*, *Zingiberis Rhizoma*, *Scutellariae Radix* and *Ephedrae Herba*) shortened the life span (Fig. 5B, Table 3A and 3B). Figure 5B showed the result using *saireito*. The crude drugs possessed a greater likelihood of decreasing life span. While the reason for the life shorting effect is still unknown, these drugs may have cytotoxicity through a variety of mechanisms, including anti-bacterial, anti-viral, detoxication or

Table 2. Growth rates of body length (A) and body width (B) of the *fer-15* mutant on NGM agar plates or in S medium containing a standard concentration of Bacto-peptone. Each value indicates the mean of three separate experiments. Approximately 25 animals were used in each experiment. Statistic comparisons of body length and width values between on NGN agar plate and in S medium were determined.

A. Body length (mm)

Concentrations of Bacto-Peptone in S medium	Days					
	1	2	3	4	5	6
x 1	0.23 ± 0.01	0.50 ± 0.01	1.01 ± 0.07	1.25 ± 0.06	1.31 ± 0.03	1.33 ± 0.06
x 2	0.23 ± 0.01	0.57 ± 0.02	1.11 ± 0.05	1.37 ± 0.04	1.46 ± 0.02	1.49 ± 0.06
x 4	0.23 ± 0.01	0.57 ± 0.02	1.14 ± 0.05	1.52 ± 0.09	1.59 ± 0.06	1.63 ± 0.09
On NGM medium	0.24 ± 0.02	0.59 ± 0.03	1.22 ± 1.47	1.47 ± 0.16	1.59 ± 0.12	1.64 ± 0.15

B. Body width (μm)

Concentrations of Bacto-Peptone in S medium	Days					
	1	2	3	4	5	6
x 1	17 ± 1	23 ± 2	42 ± 6	55 ± 2	59 ± 4	61 ± 2
x 2	17 ± 1	24 ± 2	48 ± 3	64 ± 3	69 ± 1	76 ± 5
x 4	17 ± 1	26 ± 2	51 ± 3	75 ± 6	81 ± 4	83 ± 2
On NGM medium	19 ± 2	32 ± 2	67 ± 12	81 ± 2	89 ± 2	89 ± 1

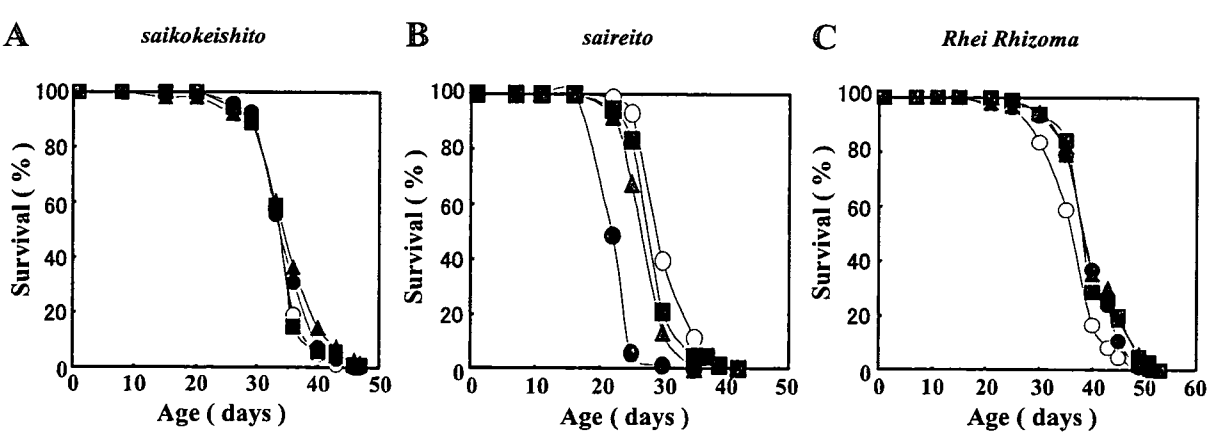

Fig 5. Life spans of a *fer-15* mutant in various kinds and concentrations of some Kampo medicines and crude drugs in S medium containing a standard concentration of Bacto-peptone. Open circles: control; Closed circles: 500 μg/ml; closed triangles: 100 μg/ml; closed squares 50 μg/ml.

Table 3. Effects of Kampo medicines (A) and crude drugs (B) on mean and maximum life spans of the *fer-15* mutant in S medium containing a standard concentration of Bacto-peptone. Effect showed effect on life span in each concentration of samples compared to control: -: shorter; ±: same ; +: longer. Statistic comparisons of mean life-span values between control and sample were determined by Tukey's multiple-range test.

A. Life spans in Kampo medicines

Name	Conc (μg/ml)	Median Life-span (days)	Maximum Life-span (days)	*p* value	Effect
daisaikoto	0	31.1	39		
	500	31.6	42	< 0.1	±
syosaikoto	0	31.1	39		
	500	32.3	44	< 0.1	±
saikokeishito	0	35.2	46		
	500	35.8	46	< 0.1	±
	100	36.2	48	< 0.1	±
	50	35.1	48	< 0.1	±
orengedokuto	0	35.2	46		
	500	30.5	40	<0.001	-
	100	33.1	46	<0.001	-
	50	33.9	46	< 0.05	-
tokishakuyakusan	0	31.3	39		
	500	30.4	39	< 0.1	±
keishibukuryogan	0	31.3	39		
	500	31.8	42	< 0.1	±
shigyakusan	0	31.3	39		
	500	32.8	43	< 0.1	±
hochuekkito	0	35.2	46		
	500	31.7	43	<0.001	-
	100	34.2	46	< 0.1	±
	50	34.1	46	< 0.1	±
rikkunshito	0	35.2	46		
	500	30.1	39	<0.001	-
	100	30.1	46	<0.001	-
	50	33.4	46	<0.005	-
shichimotsukokato	0	36.1	46		
	500	36.5	49	< 0.1	±
	100	35.1	45	< 0.1	±
	50	35.3	45	< 0.1	±
chotosan	0	36.1	46		
	500	38.0	49	<0.005	+
	100	35.8	49	< 0.1	±
	50	35.9	49	< 0.1	±
juzentaihoto	0	37.1	46		
	500	35.9	45	< 0.1	-
	100	34.6	46	< 0.05	-
	50	34.6	45	< 0.02	-
seihaito	0	36.1	46		
	500	30.0	42	<0.001	-
	100	34.5	45	< 0.02	-
	50	34.6	45	< 0.05	
daikenchuto	0	36.1	46		
	500	35.4	46	< 0.1	±
	100	36.1	45	< 0.1	±
	50	34.9	45	< 0.1	±
goshajinkigan	0	31.9	42		
	500	30.7	37	<0.005	-
	100	34.1	46	<0.002	+
	50	32.1	39	< 0.1	±
saireito	0	31.9	42		
	500	23.8	35	<0.001	-
	100	28.8	35	<0.001	-
	50	30.3	42	< 0.01	-

defervescence. Of the 26 medicines, high concentrations of *chotosan*, which is employed to treat headaches, and *Rhei Rhizoma*, which has stomach and laxative properties, expanded the life span of *C. elegans* (Fig. 5C, Table 3A and 3B). The goshajinkigan, which is employed to achieve reversal of weak physical condition in elderly people, extended the life span at a concentration of 100 μg/ml, but reduced it at 500 μg/ml. Figure 5C shows the results using *Rhei Rhizoma*. *Rhei*

Table 3 B. Life spans in crude drugs

Name	Conc. (μg/ml)	Median Life-span (days)	Maximum Life-span (days)	*p* value	Effect
Paeoniae Radix	0	32.9	39		
	500	29.7	35	<0.001	-
	100	31.9	37	< 0.1	±
	50	30.1	42	<0.01	-
Cinnamomi Cortex	0	31.9	39		
	500	21.9	44	<0.001	-
	100	28.1	37	<0.001	-
	50	27.2	39	<0.001	-
Moutan Cortex	0	35.2	47		
	500	28.4	39	<0.001	±
	100	-	-	-	
	50	32.7	47	<0.001	±
Glycyrrhizae Radix	0	35.2	47		
	500	-	-	-	-
	100	34.5	47	< 0.1	-
	50	35.0	42	< 0.1	-
Ginseng Radix	0	37.7	49		
	500	38.4	45	< 0.1	±
	100	38.4	51	< 0.1	±
	50	38.2	49	< 0.1	±
Rhei Rhizoma	0	31.2	39		
	500	33.2	45	< 0.02	+
	100	35.4	43	<0.001	+
	50	34.1	43	<0.001	+
Rhei Rhizoma	0	37.7	49		
	500	40.6	51	<0.001	+
	100	41.0	53	<0.001	+
	50	41.2	53	<0.001	+

Name	Conc. (μg/ml)	Median Life-span (days)	Maximum Life-span (days)	*p* value	Effect
Zingiberis Rhizoma	0	38.4	49		
	500	29.7	45	<0.001	-
	100	34.3	49	<0.001	-
	50	37.6	51	< 0.1	±
Bupleuri Radix	0	38.4	49		
	500	26.9	42	<0.001	±
	100	36.1	51	<0.001	±
	50	35.5	51	<0.001	±
Scutellariae Radix	0	38.4	49		
	500	22.3	30	<0.001	-
	100	23.3	30	<0.001	-
	50	30.1	45	<0.001	-
Ephedrae Herba	0	34.8	42		
	500	29.6	35	<0.001	-
	100	35.3	44	< 0.1	±
	50	34.3	44	< 0.1	±

Rhizoma in a four-fold concentration of Bacto-peptone in S medium as well as a standard concentration of Bacto-pepton also expanded the life span of *C. elegans* (data not shown). This suggests that the effect on life span is not dependent on concentration of Bacto-peptone.

3. Rhei Rhizoma is an antioxidant

Recently, much attention has been focused on the hypothesis that oxidative damage plays a role in cellular and organismal aging. It is known that some anti-oxidants expand life span of *C. elegans* (Melov *et al*, 2000; Ishii *et al*, 2004). We examined the suppressive effects of mitochondrial O_2^- by *Rhei Rhizoma*, one of the life-span enhancing medicines, to determine if the life-span extension was due to its antioxidant properties. In fact, *Rhei Rhizoma* decreased O_2^- levels, suggested that this crude drug has anti-oxidant ability (Fig. 6). We hope to isolate a single component with longevity effect from *Rhei Rhizoma* extracts using the life-span testing system described above. As *C. elegans* holds the distinction of being the first metazoan to have its genome completely sequenced and all of genes are identified (The *C. elegans* Sequencing Consortium, 1988), exam-